HHS Public Access

Author manuscript

J Appl Toxicol. Author manuscript; available in PMC 2024 May 01.

Published in final edited form as:

J Appl Toxicol. 2023 May ; 43(5): 680–693. doi:10.1002/jat.4415.

Vaping Additives Cannabinoid Oil and Vitamin E Acetate Adhere to and Damage the Human Airway Epithelium

Boris Reidel[1,2], **Sabri Abdelwahab**[1,3], **Joe Alexander Wrennall**[1,3], **Phillip Clapp**[4], **Jessica L. Beers**[5], **Klarissa D. Jackson**[5], **Robert Tarran**[1,3], **Mehmet Kesimer**[1,2,*]

[1]Marsico Lung Institute, The University of North Carolina at Chapel Hill, NC, 27599.

[2]Department of Pathology and Laboratory Medicine, The University of North Carolina at Chapel Hill, NC, 27599.

[3]Department of Cell Biology and Physiology, The University of North Carolina at Chapel Hill, NC, 27599.

[4]Department of Pediatrics, The University of North Carolina at Chapel Hill, NC, 27599.

[5]Eshelman School of Pharmacy, The University of North Carolina at Chapel Hill, NC, 27599.

Abstract

E-cigarette, or vaping product use-associated lung injury (EVALI), is a severe respiratory disorder that caused a sudden outbreak of hospitalized young people in 2019. Using cannabis oil containing vaping products, including vitamin E acetate contaminants, was found to be strongly associated with EVALI. However, the underlying tissue impacts of the condition are still largely unknown. Here, we focused on the vehicle cannabinoid oil (CBD oil) and contaminant vitamin E acetate (VEA) effects on airway epithelial cells. Primary human bronchial epithelial (HBE) cultures were exposed to e-liquid aerosols that contained CBD oil and VEA in combination or the common e-liquid components PG/VG with and without nicotine. Cell viability analysis indicated dramatically increased cell death counts after three days of CBD exposure, and this effect was even higher after CBD+VEA exposure. Microscopic examination of the cultures revealed cannabinoid and VEA depositions on the epithelial surfaces and cannabinoid accumulation in exposed cells, followed by cell death. These observations were supported by proteomic analysis of the cell secretions that exhibited increases in known markers of airway epithelial toxicity, such as xenobiotic enzymes, factors related to oxidative stress response and cell death indicators. Overall, our study provides insights into the association between cannabinoid oil and vitamin E acetate vaping and lung injury. Collectively, our results suggest that the adherent accumulation of CBD oil on airway surfaces and the cellular uptake of both CBD oil- and VEA-containing condensates cause elevated metabolomic stress, leading to increased cell death rates in human airway epithelial cultures.

*To whom correspondence should be addressed: Mehmet Kesimer, kesimer@med.unc.edu.

Author contributions:

Conception and design: MK, BR; data collection, analysis, and interpretation: BR, SA, JAW, PC, JLB, KJ, RT, MK; writing the manuscript: BR, MK.

Supplementary Table MS protein intensities:
https://figshare.com/s/18bbddc52c1fbc8b8489

Supplemental Figures:
https://figshare.com/s/197ccc5876733e2b0cfe

Short Abstract

E-cigarette, or vaping product use-associated lung injury (EVALI), is a severe respiratory disorder that caused a sudden outbreak of hospitalized young people in 2019. Despite an association with cannabinoid containing vaping products, the underlying tissue impacts of the condition remained largely unknown. Our study reveals that the adherent accumulation of CBD oil on airway surfaces and the cellular uptake of CBD oil- and VEA-containing condensates cause elevated metabolomic stress, leading to increased cell death rates in human airway epithelial cultures.

Keywords

E-cigarette; vaping; cannabinoids; vitamin E acetate; airway toxicity

Introduction:

The long-term adverse health effects of smoking are severe and impose a large burden on affected individuals and society as a whole (Warren et al., 2014). While cigarette smoking has declined in the United States in recent years (Cornelius et al., 2020; U.S.D.H.H.S, 2014), the use of electronic nicotine delivery systems (ENDS) is becoming increasingly popular (Azagba et al., 2020). The use of ENDS, particularly among younger people, has dramatically increased (up to 900%) (Murthy, 2016; Singh, Arrazola, et al., 2016) among former smokers and first-time users. ENDS are designed to aerosolize propylene glycol and glycerin e-liquids with nicotine and flavors for inhalation. However, using other substances in ENDS, such as cannabis, has become increasingly popular among younger ENDS users (Kenne et al., 2017; Miech et al., 2017; Singh, Kennedy, et al., 2016). A study by Morean et al. (Morean et al., 2015) found that 5.4% of high school students reported using cannabis in an e-cigarette.

In the second half of 2019, a dramatic increase in hospitalizations of mostly younger ENDS users approached epidemic levels, involving more than 2700 cases and resulting in over 60 deaths by February 2020 (Hartnett et al., 2020). The condition described as e-cigarette or vaping product use-associated lung injury (EVALI) is a severe respiratory disorder. Radiological imaging of EVALI patients reveals diagnoses of pneumonia, eosinophilic pneumonia, and chemical lung injury (Henry et al., 2019; Lu et al., 2020). Analysis of products used by patients revealed that cannabis oil and tetrahydrocannabinol (THC) containing vaping products, particularly from informal sources, are linked to most EVALI cases (Duffy et al., 2020; Layden et al., 2020). Furthermore, a contaminant of these cannabis oil products, vitamin E acetate (VEA), was found to be strongly associated with EVALI (Blount et al., 2019), and vitamin E acetate was found in up to 50% of the total amount in 15 tested illicit market samples (Eisenberg et al., 2019). Even though VEA was found in various products and patient samples, its pathophysiological effects on lung damage in combination with cannabinoid oils are not well understood.

In the lungs, the airway epithelium and its mucosal surface are the first points of contact for inhaled substances, and they function to protect the airways from biological and chemical hazards (Kesimer et al., 2013). In this study, we utilized the well-established model of

primary human bronchial epithelial cultures (Fulcher et al., 2005) to study the effects of CBD oil and VEA containing ENDS aerosols in contrast to common e-liquid components. Experimental conditions were chosen to replicate real-life exposure scenarios, e.g. with a VEA portion of the e-liquid of up to 50%, as reported in the analysis of products used by EVALI patients (Eisenberg et al., 2019). To assess the impacts of EVALI-associated exposure on the airway epithelium, light microscopy imaging, cytotoxicity screening and proteomics were employed. The results from this study on various compound-specific toxicity effects lead to a better understanding of EVALI pathology.

Materials and methods:

Human bronchial epithelial cell isolation and culture:

Human bronchial epithelium cells were isolated from the main stem/lobar bronchi of 6 human excess donors and excised recipient normal lung tissues were enzymatically digested following protocol #03–1396 approved by the University of North Carolina Biomedical Institutional Review Board. All methods were performed following relevant guidelines and regulations. Informed consent was obtained from all donors or authorized representatives of the donors. Cultures were used after 3–6 weeks of seeding.

Aerosol exposures:

Primary human bronchial epithelial cultures (HBECs) were isolated from 6 different normal donor lungs and grown in culture dishes. After confluence was reached (3–5 days), HBECs were maintained at an air-liquid interface (ALI) that generated polarized, well-differentiated, pseudostratified cultures resembling the *in vivo* mucociliary epithelium within 4 weeks (Pickles et al., 1998). Full-differentiated HBECs were cultured in 12-well (Ø 12 mm) culture inserts for 4 weeks and exposed in an exposure chamber apically as previously described (Clunes et al., 2008) to different PG/VG aerosol compositions or air for 3 consecutive days.

The exposures consisted of PG/VG (50%/50% vol/vol)-based aerosols that were generated using a Sigelei Fuchei 200 W Box Mod e-cigarette device with the default constant temperature setting at 450°F. A Uwell Crown stainless steel sub-tank was utilized and filled with 5 ml e-liquid per exposure session, and a 0.25-Ω SUS316 coil was used for aerosolization. The 4 investigated e-liquid compositions to generate aerosols were as follows: 1) PG/VG, 2) PG/VG containing 12 mg/ml (±)-nicotine (Sigma-Aldrich), 3) 50% PG/VG + 50% CBD oil (1000 mg Hemp Solution, Hemp Generation, Cary NC) (v/v) and 4) 50% PG/VG + 25% CBD oil + 25% vitamin E acetate (Sigma-Aldrich) (v/v/v). The CBD oil and VEA to PG/VG ratios were chosen based on mixing guides (Velvet Cloud, 2018), and observed ratios of these components found in cannabinoid-containing vaping fluids used by EVALI patients (Duffy et al., 2020). Each exposure consisted of 10 × 70 ml puffs with 30 second intervals between puffs. Aerosols and air puffs were applied apically, as depicted in Fig. 1. Apical and basal secretions were collected 2 h after a single exposure each day. On day 3, following the secretion collection, HBE cells were stained for viability assessment and analyzed using a TECAN fluorescence scanner.

Cell viability assay:

The cell viability of HBE ALI cultures exposed to air with different aerosol compositions was assessed using calcein-AM propidium iodide labeling as described in Ghosh et al., 2017 (A. Ghosh et al., 2017). Briefly, 2 h after 3 days of exposure, HBE culture secretions were collected in PBS, and cells were stained with 3 μM calcein AM (Life Technologies) in PBS apically and incubated for 30 min at 37°C. Then, the cells were washed with PBS and stained with 150 μM propidium iodide (Sigma-Aldrich) for 15 min at 37°C, which was followed by two PBS washes. The florescence intensities were quantified using an Infinite M1000 microplate reader (Tecan Trading AG). Fluorescence intensity scan were performed in technical triplicates and statistical significance was determined by Dunn's multiple comparison test.

Confocal microscopy analysis:

HBE cultures were washed apically with PBS 2 h after exposure, and the basal culture medium was exchanged. ALI cultures were then imaged on their inserts using a Leica SP8 confocal microscope (Leica Microsystems, Wetzlar, Germany) using ×10 and ×20 objective lenses. Fluorescent light fluorescence was acquired using a 405 nm diode laser with emissions collected from 410–550 nm. Microscopic analyses were performed in triplicates per exposure condition and representative images were selected for Figure 2 and 3.

Apical secretion proteomic analysis:

HBEC apical secretions were collected using 500 microliters of PBS per culture insert and were prepared for label-free quantitative proteomics. Proteomic sample preparation was performed using filter-aided sample preparation (FASP) (Wisniewski et al., 2009), including the reduction of cysteine residues by 10 mM dithiothreitol (Sigma-Aldrich) and alkylation in 50 mM iodoacetamide (Sigma-Aldrich), followed by a trypsin digestion (25 ng/μl) overnight at 37°C. The peptides were vacuum freeze-dried and dissolved in 30 μl of 2% acetonitrile and 0.1% trifluoroacetic acid, and 5 μl was injected into each sample for chromatography tandem mass spectrometry (LC-MS/MS). LC-MS/MS analysis was performed utilizing a Q-Exactive (Thermo Scientific) mass spectrometer coupled to an Ultimate 3000 nano HPLC system (Thermo Scientific), and data acquisitions were performed as described in Kesimer et al. 2015 (Kesimer et al., 2015).

Proteomic data analysis:

The raw data were processed and searched against the UniProt protein database (Homo sapiens, April 2017) using Proteome Discoverer 1.4 (Thermo Scientific) software. The following parameters were used in the Sequest search engine: 10 ppm mass accuracy for parent ions and 0.02 Da accuracy for fragment ions; 2 missed cleavages were allowed. The carbamidomethyl modification for cysteines was set to fixed, and methionine oxidation was set to variable. Scaffold 4.7.5 (Proteome Software Inc.) was used to validate the MS/MS-based peptide and protein identifications by loading individual peptide fraction data search results into MudPIT (Multidimensional Protein Identification Technology) data files for each biological sample. Peptide identifications were accepted if they had greater than 95.0% probability by the scaffold local FDR algorithm. Protein identifications were

accepted if they had greater than 99.0% probability and contained at least 2 identified peptides. Protein probabilities were assigned by the Protein Prophet algorithm (Nesvizhskii et al., 2003). Proteins that contained similar peptides and could not be differentiated based on MS/MS analysis alone were grouped to satisfy the principles of parsimony. The relative protein quantities are expressed as the total precursor intensities of all their assigned peptides. Statistical significance between the control and exposure groups was determined by Friedman's nonparametric test and Dunn's multiple comparison analysis. For quantification, the average protein intensities for 6 biological replicates were compared to determine protein level changes. Heatmap proteins were selected based on their post-2nd exposure relative abundance difference between PG/VG and PG/VG + CBD oil + VEA by the Wilcoxon signed rank test. The heatmap was generated using the software tool Heatmapper (Babicki et al., 2016).

Aerosol particle size analysis:

An eight-stage Sierra Series 210 Cascade Impactor (Sierra Instruments, Carmel Valley, CA) was operated with an airflow rate of 14 l/min to determine the particle size distributions. This flow rate is one of the recommended flow rates for operation and the stage cutoff sizes are clearly provided. The 50% collection efficiency for the impactor stages spans aerodynamic diameters from 0.15 to 13 μm at 14 l/min. Prior to each run, filter paper was weighed using a microbalance, and each filter's weight and designated stage were recorded. A Sigelei Fuchai 213 box-mod device and Crown II tank were used at a 40 W power setting to generate aerosols of 50:50 PG/VG, 50:50 PG/VG containing 50% CBD, or 50:50 PG/VG containing 25% CBD and 25% vitamin E acetate (VEA). Each aerosol test was conducted within a chemical fume hood and began with 10 seconds of ambient air followed by a single 5-second puff and then an additional 10 seconds of ambient air. Following each test, filter papers were weighed a second time to assess particle deposition at each stage, and masses were then used to calculate the aerosol particle mass median aerodynamic diameter (MMAD) and the geometric standard deviation (GSD). The MMAD and GSD were calculated using the probit method as previously described by Hinds (Hinds). Accordingly, the probit method plots the cumulative mass percent versus the related mean cutoff diameter of each stage of the impactor on a log probability graph. Thus, the aerodynamic diameter associated with a cumulative count of 50% (d50%) corresponds to MMAD, while GSD is estimated. Samples were analyzed in triplicate repeats and ANOVA statistical analysis was performed to compare aerosol MMADs.

Cannabinoid chemical analysis:

A certified reference standard containing 1 mg/ml each of (−)-Δ^9-THC, cannabinol (CBN) and cannabidiol (CBD) in methanol was purchased from Cerilliant (Round Rock, TX). The internal standard CBD-d_9 (1 mg/mL in methanol) was purchased from Cayman Chemical (Ann Arbor, MI). Hemp oil samples were diluted 1:2000 in 1:1 methanol: water, centrifuged at 4,000 rpm for 20 min, and analyzed using a Thermo TSQ Quantum Ultra triple quadrupole mass spectrometer coupled to a Waters Acquity UPLC system. A 50 × 2.1 mm Phenomenex Kinetex EVO C18 column with a 2.6 μm particle size maintained at 40°C was used for analysis. A gradient elution scheme was used for compound separation, where eluent A was 5% methanol in water with 0.1% acetic acid and eluent B was 5% methanol

in acetonitrile with 0.1% acetic acid: 60% A from 0 to 0.7 min, 60% A to 10% A from 0.7 to 2.1 min, 10% A from 2.1 to 2.5 min, 10% A to 60% A from 2.5 to 2.6 min, and 60% A from 2.6 to 4 min. Selected reaction monitoring was used in negative ion mode with the following precursor-to-product ion transitions and collision energies for detection and quantitation: m/z 313 > 245 and m/z 313 > 191 for CBD and THC (26 V), m/z 322 > 254 for CBD-d_9 (internal standard) (27 V), and m/z 309 > 279 for CBN (30 V).

Results:

EVALI is strongly associated with the vaping of cannabinoids. To investigate how aerosols that contain cannabinoid oil and the contaminant vitamin E acetate may impact airway surfaces, we exposed primary HBECs established from six nonsmoker donors to different aerosol compositions or air on three consecutive days (Fig. 1) and analyzed the airway epithelial viability, morphology and apical secretion composition, in addition to aerosol particle size.

Cannabinoid oil compound analysis:

To verify the amounts of the most common cannabinoids in the CBD oil used for exposures, we subjected CBD oil samples to LC-MS/MS analysis and used (labeled) standards for quantification. Supplementary Fig. 1 shows the representative chromatograms of the cannabinoid oil components cannabidiol (CBD), tetrahydrocannabinol (THC) and cannabinol (CBN). The quantification results of these 3 compounds using standard curves are presented in Suppl. Figure 2 and Suppl. Table 1. The measured amounts of CBD (26.2 ± 1.6 mg/ml), THC (1.90 ± 0.46 mg/ml) and CBN (63.9 ± 18.5 μg/ml) were within ranges provided the manufacturer and therefore classify the products as a hemp or cannabinoid oil.

Cannabinoid oil and vitamin E acetate aerosol condensates accumulate in and on airway epithelial cells and lead to cell death:

Following cannabinoid oil and VEA-containing aerosol exposure, HBECs were examined daily by light microscopy. Figure 2 shows the microscopic images of HBECs 22 h after the first aerosol exposure and two hour prior to the 2 day exposures. In the overview examination using a x 10 objective lens, we observed confluent and homogeneous cell layers for the air- and PG/VG plus nicotine-exposed cultures (Fig. 2A and C). In contrast, CBD oil-exposed cultures and CBD oil plus VEA-exposed cultures showed apparent accumulation of visible condensation droplets on the apical surface of HBECs (Fig. 2 D and E). Only the VEA-exposed culture surfaces showed smaller droplet accumulations 22 h after exposure (the white arrow in Fig. 2E) that were distinct and smaller in size than the droplets observed on HBE cultures exposed to CBD oil aerosol alone (the black arrow in Fig. 2D). HBECs exposed to PG/VG-only aerosol displayed no apparent accumulation of such droplets but presented a less homogenous cell layer than that of the air controls and PG/VG+N-exposed cultures.

To acquire information on the contents of the observed aerosol condensate droplets by light microscopy (Fig. 3), we took advantage of the known fluorescent properties of cannabinoids that show an excitation maximum wavelength of approximately 370 nm and

an emission maximum wavelength of approximately 420 nm (Dienyssiou-Asteriou & Miras, 1975). PG/VG alone showed no visible fluorescence at 370 nm excitation and 420 nm emission wavelengths compared to that of the acetonitrile solvent. PG/VG CBD oil had the highest fluorescence signal, and PG/VG CBD oil + VEA showed roughly half of that intensity, which agrees with the result of containing 50% less cannabinoid oil. We then microscopically examined HBECs two hours after the 2nd day of exposure by using fluorescent light to identify the accumulation of cannabinoids. Using UV laser excitation and an emission window of 410–550 nm, the rounded culture areas visibly distinct in transmission light after CBD oil exposure also showed a fluorescence signal (Fig. 3A and B). Prior to the microscopy fluorescence imaging, we measured the fluorescence of our exposure e-liquids PG/VG, PG/VG CBD oil mix and PG/VG CBD oil VEA mix, each diluted 1:10 in acetonitrile using a plate reader fluorescence scanner (Fig. 3C). In addition to the HBECs areas that formed rounded and dome-shaped areas with a centric fluorescence signal, fluorescence was also detected within smaller surface accumulation droplets on the PG/VG+CBD+VEA-exposed cultures (Fig. 3D–F). The culture areas with cannabinoid fluorescence signal accumulation also displayed cell density and morphology loss (Fig. 3A, D and F). These visual indications of the viability decreased in the cultures exposed to PG/VG+CBD and PG/VG+CBD+VEA after 2 day exposures were confirmed by life/death staining assays, which showed high cell death rates of approximately 45% and 60%, respectively, after 3 day exposures, as opposed to the 1% to 3% rates seen in the other exposure conditions (Fig. 4).

To investigate whether the toxicity of the CBD oil- and VEA-containing aerosols could be related to a difference in aerosol deposition due to aerosol particle sizes, we analyzed the particle sizes of CBD oil-, VEA-containing and PG/VG-alone aerosols (Suppl. Fig. 3). This analysis showed that the aerosol particles of the compared compositions did not have significantly different sizes.

Cannabinoid oil and vitamin E acetate aerosols impact the integrity of the airway epithelial cell layer and change the protein composition of the apical surface liquid:

To investigate the impacts CBD oil- and VEA-containing aerosols have on the integrity and homeostasis of airway epithelium in more detail, we analyzed the apical secretions of aerosol-exposed HBECs by label-free quantitative proteomics. Samples were collected every day 2 h after consecutive daily exposures and analyzed by LC-MS/MS. By setting a peptide confidence interval of 95% and requiring a minimum of 2 assigned peptides per protein, our proteomic analysis of HBEC apical secretions identified a total of approximately 2000 proteins across all analyzed samples (Supplementary Data). For an initial assessment of the impact of the different exposures on the secretion composition, the number of uniquely identified proteins per group was compared using Venn diagrams (Fig. 5). Since all aerosols used in this study contained at least 50% PG/VG, we first evaluated the global proteome changes induced by PG/VG alone and PG/VG containing 12 mg/ml nicotine (Fig. 5A). 281 unique proteins were identified in the secretions from HBECs exposed to PG/VG aerosol post day 1 exposure, with some overlap of the uniquely identified proteins in the PG/VG+N exposed cultures. This overlap increased after consecutive exposures and displayed the highest numbers of uniquely identified proteins that were shared between

PG/VG and PG/VG+N post-2 day (310 proteins) and post-3 day (286 proteins) exposures (Fig. 5A). To discriminate between effects of CBD oil- and VEA-containing aerosols from the baseline effects seen by PG/VG alone, the numbers of uniquely identified proteins from these three groups were presented in Figure 5B. The largest number of unique proteins was identified in the PG/VG group after the day 1 exposure. However, there was a shift toward highest unique proteins numbers after the 2 day and 3 day exposures in the PG/VG+CBD+VEA (and PG/VG overlapping) identifications. This trend also indicates that the set of proteins that appeared in the apical secretions in response to PG/VG+CBD+VEA over days 2 and 3 is different from the PG/VG set of unique proteins. To gain some insight into the functional differences of the unique protein sets after PG/VG alone and VEA, we performed a PANTHER (Thomas et al., 2003) protein classification analysis (Suppl. Fig. 4). This analysis indicated that there were several shifts regarding the representation of protein classes between the PG/VG alone and VEA-containing exposures. For the VEA-exposed cultures, these shifts include reductions in IDs among protein modifying enzymes and transmembrane signal receptors and strongly increased numbers of translational proteins and nucleic acid metabolism proteins compared to that of PG/VG alone.

To examine whether the increased presence of cytosolic proteins in the apical secretions of exposed cultures was accompanied by the loss of epithelial integrity, we quantified the apical abundance of two proteins that are exclusive to the basolateral culture medium and not expressed by HBECs. Accordingly, serotransferrin (TF) and serum albumin (ALB) were significantly increased in apical secretions of VEA-exposed cultures after 2 day exposures and in CBD oil and VEA after 3 day exposures, signifying an epithelial barrier loss that was not observed among the other exposure groups (Fig. 6). This result largely parallels the cytotoxicity assessment, in which increased cell death rates were detected after the day 3 CBD oil (45%) and VEA (60%) aerosol exposure, significantly contributing to this leakage (Fig. 4).

The extracellular presence of cytosolic metabolism enzymes is often utilized as a measure to assess cytotoxicity. Fig. 7 shows the intensities of two commonly employed cytotoxicity markers, glyceraldehyde-3-phosphate dehydrogenase (GAPDH) and lactate dehydrogenase (LDH), across all conditions and exposure days. GAPDH and LDH displayed significantly increased levels after the day 3 exposure to PG/VG and PG/VG+N, while CBD and VEA exposures led to peak extracellular levels of these enzymes after the day 2 exposure, indicating that there was an earlier toxicity impact.

To visualize the aerosol exposure-dependent changes in the protein abundances of the apical lining fluid, a heatmap was generated (Fig. 8). The heatmap contains the set of proteins that demonstrated significantly changed levels after VEA exposure compared to that of PG/VG alone following the 2 day exposures. This representation illustrates that there are clusters of proteins that display similar abundance changes among exposures as well as clusters of proteins with very exposure-specific changes. Three of these clusters are highlighted by rectangles in Figure 8 that are labeled I, II and III. Cluster I comprises proteins that are particularly increased after CBD exposure compared to that of all other groups, although it has some similarity to VEA exposure. A STRING protein interaction network analysis of this protein subset included the following distinct pathways: glycan degradation and

carbon metabolism (Suppl. Fig. 5). Cluster II represented the largest group of proteins with decreased levels in the CBD- and VEA-exposed cultures. The STRING analysis focused on cellular localization indicated that the majority (39 of 60) of the proteins in this cluster were typically extracellular (Suppl. Fig. 6), which highlighted a general trend of reduced protein apical secretion after CBD and VEA exposure.

Figure 9 shows the relative abundances of the following exemplary secreted airway epithelial proteins: BPI fold containing family B member 1 (BPIFB1), mucin 4 (MUC4), galectin 3 binding protein (LG3BP) and secretory leukocyte peptidase inhibitor (SLPI), all of which displayed significant reductions after CBD and VEA 2 day exposures.

Cluster III of the heatmap (Fig. 8) contains proteins with similarly increased levels after VEA aerosol exposure that comprise glycolytic and amino acid biosynthesis enzymes, as well as ribosomal proteins (Suppl. Fig. 7). The strong presence of ribosomal and mitochondrial proteins after the 2nd VEA aerosol exposure was distinct from all other groups, including CBD exposures. Among the sets of proteins that showed significant increases after the 2nd CBD exposure were detoxification and redox balance enzymes such as glutathione S-transferase P1 (GSTP1) and superoxide dismutase 1 (SOD1) as well as the xenobiotic target protein (SELENBP1) (Fig. 10).

Discussion:

The causative pathological mechanisms in EVALI are still largely unknown; however, the use of cannabinoid oil containing vaping products and the contaminant vitamin E acetate were found to be strongly associated with EVALI (Duffy et al., 2020; Layden et al., 2020). Since in the past neither nicotine vaping nor the use of THC had been described to cause acute lung injuries as observed in EVALI, and largely varying amounts of Delta9-THC detected in product samplings of EVALI cases (Guo et al., 2021), we focused our study on freely available CBD oil that contains the same most common carrier solvent (medium-chain triglycerides oil) for cannabinoids as is the case for THC vaping products. Since the cannabinoid vaping liquid additive vitamin E acetate has been shown to be highly associated with EVALI (Blount et al., 2020), we aimed our airway epithelial toxicity analyses on these two major common components identified in EVALI cases. VEA alone was not tested to replicate real-life exposure scenarios, since pure VEA aerosols have a much smaller particle size than PG/VG aerosols (Mikheev et al., 2020), which affects its deposition to cell surfaces and thereby would have compromised the comparability of our measured outcomes, also in regards to real-live exposure. First, we analyzed the composition of the cannabinoid oil used in our aerosol exposure contaminants (Suppl. Fig. 1, 2, and Suppl. Table 1). These analyses confirmed that the amounts of CBD, CBN and THC were within the ranges of concentrations provided by the manufacturer and ensured that the potential observed effects were independent of THC.

To gain insights into the pathological effects of cannabinoid oil vaping on the airways, we exposed human airway epithelial cultures to PG/VG aerosols containing cannabinoid oil and VEA (Fig. 1). Our studies revealed several novel insights. First, 24 h after exposure, CBD oil- and VEA-containing aerosol condensates accumulated on the surface of HBECs,

in contrast to no visible accumulations of the common e-liquid PG/VG (Fig. 2). This observation agrees with findings by Blount et al. who detected vitamin E acetate in bronchoalveolar lavage fluids in 94% of their EVALI cohort (Blount et al., 2019). Indeed, we were able to observe oily droplet accumulations prior to the day 2 exposures and the daily apical wash of the airway surface, which indicated that accumulations persisted at least 24 h after exposure and may contribute to the EVALI pathology.

In fact, our imaging analysis post 2-day exposures shows that HBECs contained CBD oil after aerosol exposure, which led to the affected fluorescent areas of the cultures swelling and displaying nonuniform cells and confluence reduction (Fig. 3). These indications of nonhealthy cell areas ultimately resulted in high levels (~45%) of cell death after day 3 (Fig. 4). A similar decrease in cell viability of airway epithelial cell cultures was observed by Leigh et al. after exposure to propylene glycol based cannabidiol containing aerosols (Leigh & Goniewicz, 2020). Further, CBD+VEA exposed culture surfaces displayed cannabinoid fluorescence droplets. The addition of VEA may contribute to these droplets persisting on the apical surface (Fig. 3F). Cultures exposed to VEA-containing aerosols showed even higher levels of dead cells (~60%) after the third exposure (Fig. 4). A cellular uptake or absorption of aerosolized VEA has also been observed in human alveolar epithelial type II cells and lead to increased cell death (Matsumoto et al., 2020). These findings may indicate that airway epithelial cells can be overburdened with the clearance of hemp oil condensates, since lung tissue typically lacks the major cytochrome P450 metabolomic enzymes CYP2C19 and CYP3A4 that are involved in the breakdown of CBD as well as VEA (Zendulka et al., 2016).

In previous studies we have demonstrated that, our apical airway proteomic analyses correlate well with individual proteins measurements and are a valuable tool to globally assess toxicity effects of tobacco product use on the airways (Ghosh et al., 2017; Abdelwahab et al., 2020). To further characterize the effects of CBD and VEA aerosols on the airway surface, we collected apical lining fluid samples of HBE cultures daily two hours after exposure and analyzed the protein composition by LC-MS/MS. First, the results of this analysis unexpectantly showed that PG/VG aerosol-only exposures displayed an early impact on the number of changing proteins compared to that of air that was not mirrored by PG/VG+N exposures (Fig. 5A). This may be related to a nicotine effect that initially increases the permeability of the airway epithelial cell layer, which facilitates less PG/VG aerosol condensate accumulation on the apical surface. This hypothesis is supported by our relative quantification of the basal media; only the proteins albumin and serotransferrin showed increased apical leakage after nicotine-containing aerosol exposure (Fig. 6). Furthermore, this permeability-increasing effect of nicotine-containing PG/VG has also been observed by others (B. Ghosh et al., 2020). Furthermore, another important observation was made on the impact of PG/VG only exposures that showed relatively high numbers of uniquely identified proteins with intracellular origins. Since the observed protein number increases found in apical secretion were not accompanied by increased cell death rates (Fig. 4), these increases likely stemmed from PG/VG-induced cytosolic leakage, which has also been observed by others in the form of cell shrinkage (Woodall et al., 2020). In contrast, the apical secretome changes after CBD oil, particularly after CBD oil+VEA exposure (Fig. 5B), were associated with high cell death rates on day 3. This loss in cell

viability was indicated after the 2nd exposure by strong increases in translational and nucleic acid metabolism proteins in CBD and VEA samples that were absent from cultures exposed to PG/VG alone (Fig. 8 and Suppl. Fig. 4).

Since aerosol particle size measurements (Suppl. Fig. 6) did not indicate differences between PG/VG alone and CBD oil- or VEA-containing aerosols, the observed toxic effects are unlikely to be a result of changed deposition. Rather, the effects likely resulted from accumulations on and in the airway epithelium that led to cellular damage (Fig. 3). This cell damaging effect is demonstrated through the integrity loss of the epithelium shown by leakage of the basal media proteins albumin and serotransferrin after the second and third exposures (Fig. 6) and correlates with dramatic increases in dead cells after day 3 that are absent in the control groups such as PG/VG alone (Fig. 4).

This drop in viability of CBD- and VEA-exposed cultures on day 3 is also reflected in the reduced amounts of cytosolic proteins, such as GAPDH and LDHB, at day 3 compared to day 2 (Fig. 7), which was likely due to decreased protein synthesis. We concluded that the total cell numbers had already decreased substantially by day 3 in CBD and VEA treated cultures due to strong toxicity effects leading to overall lower protein levels than on day 2. While exposure to PG/VG resulted in cytosolic proteins, such as GAPDH or LDHB peaking at day 3 in the apical lining fluid of exposed HBECs (Fig. 7), PG/VG exposure did not result in significantly increased cell death (Fig. 4). These differential patterns of aerosol composition-specific protein level changes are further illustrated in the heatmap of Figure 8. Among several clusters in this heatmap, the following clusters that characterized different toxicity outcomes were significant: Group I included proteins with similar increases after CBD exposure that were associated with the processes of glycan degradation and carbon metabolism (Suppl. Fig. 6). Exposure to CBD aerosols was associated with increases in proteins that play a role in detoxification and redox stress (Fig. 10), which have also been observed in response to cigarette smoke in airway secretions in vitro and *in vivo* (Abdelwahab et al., 2020; A. Ghosh et al., 2017; Reidel et al., 2018). In addition, CBD exposure also led to increases in proteins that are targets and responders to natural xenobiotics (Fang et al., 2009), such as SELENBP1 (Fig. 10C).

In contrast, Group II contained mitochondrial, ribosomal, and amino acid biosynthesis proteins that were similarly increased after VEA exposure (Suppl. Fig. 8). These results hint at the different toxicity effects of CBD alone and VEA on airway epithelial cells. The degradation of ribosomes and mitochondria and the release of intracellular content are features of necrosis (Cummings & Schnellmann, 2004; Marshall et al., 2014) that were not pronounced after CBD exposure at day 2 and may indicate accelerated cell death after VEA exposure. Group II indicated a general trend that was observable among both protein compositional changes of CBD and CBD plus VEA exposures versus the remaining control groups, which was a significant and broad decrease in major secreted proteins (Fig. 8 and 9). Besides these proteomic cell viability decrease indicators, VEA exposure has also been shown to increase cysteinyl leukotrienes, such as LTC4 and LTE4 (Muthumalage et al., 2020), which are potent bronchoconstrictors and stimulators of mucus secretion that may further exacerbate the EVALI condition. It should be noted that, the extend of toxicity effects of CBD oil and VEA vapors observed in our *in vitro* system may differ from the

severity *in vivo,* where additional protective mechanisms such as immune cell responses and mucociliary clearance are at work. Nonetheless, our analysis delivers insights towards the nature of the toxicity insults of the investigated exposures and thereby aids in the understanding of the pathological outcomes observed in patients.

Taken together, the microscopic imaging and cell viability outcomes observed are supported by the results of our proteomic analysis of HBEC apical lining fluid that showed dramatic changes in their protein compositions following CBD oil and VEA aerosol exposure. After 2 consecutive exposures to CBD- and VEA-containing aerosols in 24-h intervals, HBECs displayed cannabinoid material accumulation and severe cell layer displacement that resulted in high cell death rates by day 3. While VEA exposure displayed the strongest effect on airway cells and caused necrosis resembling proteome changes during cell death, CBD oil exposure alone also had strong impacts on airway epithelial cultures by reducing integrity and viability.

To our knowledge, this is the first study utilizing primary human bronchial epithelial cultures that demonstrates the airway surface effects of EVALI-associated ENDS aerosols and their cellular toxicity outcomes. Our study strengthens the hypothesis of a cumulative EVALI pathology of oxidative and metabolomic stress inducing CBD oil compounds and a toxic airway surface coating effect by VEA. Taken together, these airway epithelium-damaging factors likely play significant roles in the overall EVALI pathology and build an argument to strongly advise against the inhalation of CBD oil containing e-liquids, particularly from ambiguous sources.

Supplementary Material

Refer to Web version on PubMed Central for supplementary material.

Acknowledgments

This work was funded by NIH/FDA grants P50HL120100, R03HL140402-01A1 and R01HL135642. Research reported in this publication was supported by NIH and the Family Smoking Prevention and Tobacco Control Act. The content is solely the responsibility of the authors and does not necessarily represent the official views of the NIH or the Food and Drug Administration. The authors thank Biostatistician Agathe Ceppe for assisting with statistical analyses.

Availability of materials and data:

All data generated or analysed during this study are included in this published article [and its supplementary information files] and are available from the corresponding author on reasonable request.

References

Abdelwahab SH, Reidel B, Martin JR, Ghosh A, Keating JE, Haridass P, . . . Kesimer M (2020). Cigarillos Compromise the Mucosal Barrier and Protein Expression in Airway Epithelia. American journal of respiratory cell and molecular biology, 63(6), 767–779. doi:10.1165/rcmb.2019-0085OC [PubMed: 32877614]

Azagba S, Manzione L, Shan L, & King J (2020). Trends in Smoking Behaviors Among US Adolescent Cigarette Smokers. Pediatrics, 145(3). doi:10.1542/peds.2019-3047

Babicki S, Arndt D, Marcu A, Liang Y, Grant JR, Maciejewski A, & Wishart DS (2016). Heatmapper: web-enabled heat mapping for all. Nucleic acids research, 44(W1), W147–153. doi:10.1093/nar/gkw419 [PubMed: 27190236]

Blount BC, Karwowski MP, Morel-Espinosa M, Rees J, Sosnoff C, Cowan E, . . . Pirkle JL (2019). Evaluation of Bronchoalveolar Lavage Fluid from Patients in an Outbreak of E-cigarette, or Vaping, Product Use-Associated Lung Injury - 10 States, August-October 2019. Morbidity and mortality weekly report, 68(45), 1040–1041. doi:10.15585/mmwr.mm6845e2 [PubMed: 31725707]

Blount BC, Karwowski MP, Shields PG, Morel-Espinosa M, Valentin-Blasini L, Gardner M, . . . Group LIRLW (2020). Vitamin E Acetate in Bronchoalveolar-Lavage Fluid Associated with EVALI. New England Journal of Medicine, 382(8), 697–705. doi:10.1056/NEJMoa1916433 [PubMed: 31860793]

Clunes LA, Bridges A, Alexis N, & Tarran R (2008). In vivo versus in vitro airway surface liquid nicotine levels following cigarette smoke exposure. Journal of analytical toxicology, 32(3), 201–207. [PubMed: 18397571]

Cornelius ME, Wang TW, Jamal A, Loretan CG, & Neff LJ (2020). Tobacco Product Use Among Adults - United States, 2019. Morbidity and mortality weekly report, 69(46), 1736–1742. doi:10.15585/mmwr.mm6946a4 [PubMed: 33211681]

Cummings BS, & Schnellmann RG (2004). Measurement of cell death in mammalian cells. Current protocols in pharmacology, Chapter 12, Unit 12 18. doi:10.1002/0471141755.ph1208s25

Dienyssiou-Asteriou A, & Miras CJ (1975). Fluorescence of cannabinoids. The Journal of pharmacy and pharmacology, 27(2), 135–136. doi:10.1111/j.2042-7158.1975.tb09424.x [PubMed: 237076]

Duffy B, Li L, Lu S, Durocher L, Dittmar M, Delaney-Baldwin E, . . . Spink D (2020). Analysis of Cannabinoid-Containing Fluids in Illicit Vaping Cartridges Recovered from Pulmonary Injury Patients: Identification of Vitamin E Acetate as a Major Diluent. Toxics, 8(1). doi:10.3390/toxics8010008

Eisenberg Z, Moy D, Lam V, Cheng C, Richard J, & Burack B (2019). Contaminant analysis of illicit vs regulated market extracts. Rettrieved from: https://anresco.com/contaminant-analysis-of-illicit-vs-regulated-market-extracts/

Fang J, Koen YM, & Hanzlik RP (2009). Bioinformatic analysis of xenobiotic reactive metabolite target proteins and their interacting partners. BMC chemical biology, 9, 5. doi:10.1186/1472-6769-9-5 [PubMed: 19523227]

Fulcher ML, Gabriel S, Burns KA, Yankaskas JR, & Randell SH (2005). Well-differentiated human airway epithelial cell cultures. Methods in molecular medicine, 107, 183–206. [PubMed: 15492373]

Ghosh A, Abdelwahab SH, Reeber SL, Reidel B, Marklew AJ, Garrison AJ, . . . Tarran R (2017). Little Cigars are More Toxic than Cigarettes and Uniquely Change the Airway Gene and Protein Expression. Scientific reports, 7, 46239. doi:10.1038/srep46239 [PubMed: 28447619]

Ghosh B, Reyes-Caballero H, Akgun-Olmez SG, Nishida K, Chandrala L, Smirnova L, . . . Sidhaye VK (2020). Effect of sub-chronic exposure to cigarette smoke, electronic cigarette and waterpipe on human lung epithelial barrier function. BMC pulmonary medicine, 20(1), 216. doi:10.1186/s12890-020-01255-y [PubMed: 32787821]

Guo W, Vrdoljak G, Liao VC, & Moezzi B (2021). Major Constituents of Cannabis Vape Oil Liquid, Vapor and Aerosol in California Vape Oil Cartridge Samples. Frontiers in Chemistry, 9, 694905. doi:10.3389/fchem.2021.694905 [PubMed: 34368078]

Hartnett KP, Kite-Powell A, Patel MT, Haag BL, Sheppard MJ, Dias TP, . . . Adjemian J (2020). Syndromic Surveillance for E-Cigarette, or Vaping, Product Use-Associated Lung Injury. The New England journal of medicine, 382(8), 766–772. doi:10.1056/NEJMsr1915313 [PubMed: 31860794]

Henry TS, Kanne JP, & Kligerman SJ (2019). Imaging of Vaping-Associated Lung Disease. The New England journal of medicine, 381(15), 1486–1487. doi:10.1056/NEJMc1911995 [PubMed: 31491070]

Hinds WC Aerosol technology : properties, behavior, and measurement of airborne particles (2nd ed.).

Kenne DR, Fischbein RL, Tan AS, & Banks M (2017). The Use of Substances Other Than Nicotine in Electronic Cigarettes Among College Students. Substance abuse : research and treatment, 11, 1178221817733736. doi:10.1177/1178221817733736 [PubMed: 28979131]

Kesimer M, Cullen J, Cao R, Radicioni G, Mathews KG, Seiler G, & Gookin JL (2015). Excess Secretion of Gel-Forming Mucins and Associated Innate Defense Proteins with Defective Mucin Un-Packaging Underpin Gallbladder Mucocele Formation in Dogs. PloS one, 10(9), e0138988. doi:10.1371/journal.pone.0138988 [PubMed: 26414376]

Kesimer M, Ehre C, Burns KA, Davis CW, Sheehan JK, & Pickles RJ (2013). Molecular organization of the mucins and glycocalyx underlying mucus transport over mucosal surfaces of the airways. Mucosal immunology, 6(2), 379–392. doi:10.1038/mi.2012.81 [PubMed: 22929560]

Layden JE, Ghinai I, Pray I, Kimball A, Layer M, Tenforde MW, . . . Meiman J (2020). Pulmonary Illness Related to E-Cigarette Use in Illinois and Wisconsin - Final Report. The New England journal of medicine, 382(10), 903–916. doi:10.1056/NEJMoa1911614 [PubMed: 31491072]

Leigh NJ, & Goniewicz ML (2020). Effect of aerosolized nicotine on human bronchial epithelial cells is amplified after co-administration with cannabidiol (CBD): a pilot in vitro study. BMC Pharmacology and Toxicology, 21(1), 42. doi:10.1186/s40360-020-00418-1 [PubMed: 32498718]

Lu MA, Jabre NA, & Mogayzel PJ Jr. (2020). Vaping-related Lung Injury in an Adolescent. American journal of respiratory and critical care medicine, 201(4), 481–482. doi:10.1164/rccm.201909-1786IM [PubMed: 31904992]

Marshall KD, Edwards MA, Krenz M, Davis JW, & Baines CP (2014). Proteomic mapping of proteins released during necrosis and apoptosis from cultured neonatal cardiac myocytes. American journal of physiology. Cell physiology, 306(7), C639–647. doi:10.1152/ajpcell.00167.2013 [PubMed: 24401845]

Matsumoto S, Fang X, Traber MG, Jones KD, Langelier C, Hayakawa Serpa P, . . . Gotts JE (2020). Dose-Dependent Pulmonary Toxicity of Aerosolized Vitamin E Acetate. American Journal of Respiratory Cell and Molecular Biology, 63(6), 748–757. doi:10.1165/rcmb.2020-0209OC [PubMed: 32822237]

Miech R, Patrick ME, O'Malley PM, & Johnston LD (2017). What are kids vaping? Results from a national survey of US adolescents. Tobacco control, 26(4), 386–391. doi:10.1136/tobaccocontrol-2016-053014 [PubMed: 27562412]

Mikheev VB, Klupinski TP, Ivanov A, Lucas EA, Strozier ED, & Fix C (2020). Particle Size Distribution and Chemical Composition of the Aerosolized Vitamin E Acetate. Aerosol Science and Technology, 54(9), 993–998. doi:10.1080/02786826.2020.1783431 [PubMed: 33132476]

Morean ME, Kong G, Camenga DR, Cavallo DA, & Krishnan-Sarin S (2015). High School Students' Use of Electronic Cigarettes to Vaporize Cannabis. Pediatrics, 136(4), 611–616. doi:10.1542/peds.2015-1727 [PubMed: 26347431]

Murthy VH (2016). E-Cigarette Use Among Youth and Young Adults: A Major Public Health Concern. JAMA pediatrics. doi:10.1001/jamapediatrics.2016.4662

Muthumalage T, Lucas JH, Wang Q, Lamb T, McGraw MD, & Rahman I (2020). Pulmonary Toxicity and Inflammatory Response of E-Cigarette Vape Cartridges Containing Medium-Chain Triglycerides Oil and Vitamin E Acetate: Implications in the Pathogenesis of EVALI. Toxics, 8(3). doi:10.3390/toxics8030046

Nesvizhskii AI, Keller A, Kolker E, & Aebersold R (2003). A statistical model for identifying proteins by tandem mass spectrometry. Analytical chemistry, 75(17), 4646–4658. [PubMed: 14632076]

Pickles RJ, McCarty D, Matsui H, Hart PJ, Randell SH, & Boucher RC (1998). Limited entry of adenovirus vectors into well-differentiated airway epithelium is responsible for inefficient gene transfer. Journal of Virology, 72(7), 6014–6023. [PubMed: 9621064]

Reidel B, Radicioni G, Clapp P, Ford AA, Abdelwahab S, Rebuli ME, . . . Kesimer M (2018). E-Cigarette Use Causes a Unique Innate Immune Response in the Lung Involving Increased Neutrophilic Activation and Altered Mucin Secretion. American journal of respiratory and critical care medicine. doi:10.1164/rccm.201708-1590OC

Singh T, Arrazola RA, Corey CG, Husten CG, Neff LJ, Homa DM, & King BA (2016). Tobacco Use Among Middle and High School Students--United States, 2011–2015. Morbidity and mortality weekly report, 65(14), 361–367. doi:10.15585/mmwr.mm6514a1 [PubMed: 27077789]

Singh T, Kennedy S, Marynak K, Persoskie A, Melstrom P, & King BA (2016). Characteristics of Electronic Cigarette Use Among Middle and High School Students - United States, 2015. Morbidity and mortality weekly report, 65(50–51), 1425–1429. doi:10.15585/mmwr.mm655051a2 [PubMed: 28033310]

Thomas PD, Kejariwal A, Campbell MJ, Mi H, Diemer K, Guo N, . . . Doremieux O (2003). PANTHER: a browsable database of gene products organized by biological function, using curated protein family and subfamily classification. Nucleic acids research, 31(1), 334–341. [PubMed: 12520017]

U.S.D.H.H.S. (2014). The Health Consequences of Smoking—50 Years of Progress. A Report of the Surgeon General. Retrieved from Atlanta, GA:

Cloud Velvet. (2018). A Guide to Mixing Cannabis and CBD Oils with E-Liquids. Retrieved from https://velvetcloud.com/blogs/news/a-guide-to-mixing-cannabis-and-cbd-oils-with-e-liquids

Warren GW, Alberg AJ, Kraft AS, & Cummings KM (2014). The 2014 Surgeon General's report: "The health consequences of smoking−-50 years of progress": a paradigm shift in cancer care. Cancer, 120(13), 1914–1916. doi:10.1002/cncr.28695 [PubMed: 24687615]

Wisniewski JR, Zougman A, Nagaraj N, & Mann M (2009). Universal sample preparation method for proteome analysis. Nature methods, 6(5), 359–362. doi:10.1038/nmeth.1322 [PubMed: 19377485]

Woodall M, Jacob J, Kalsi KK, Schroeder V, Davis E, Kenyon B, . . . Baines DL (2020). E-cigarette constituents propylene glycol and vegetable glycerin decrease glucose uptake and its metabolism in airway epithelial cells in vitro. American journal of physiology. Lung cellular and molecular physiology, 319(6), L957–L967. doi:10.1152/ajplung.00123.2020 [PubMed: 32996783]

Zendulka O, Dovrtelova G, Noskova K, Turjap M, Sulcova A, Hanus L, & Jurica J (2016). Cannabinoids and Cytochrome P450 Interactions. Current drug metabolism, 17(3), 206–226. doi:10.2174/1389200217666151210142051 [PubMed: 26651971]

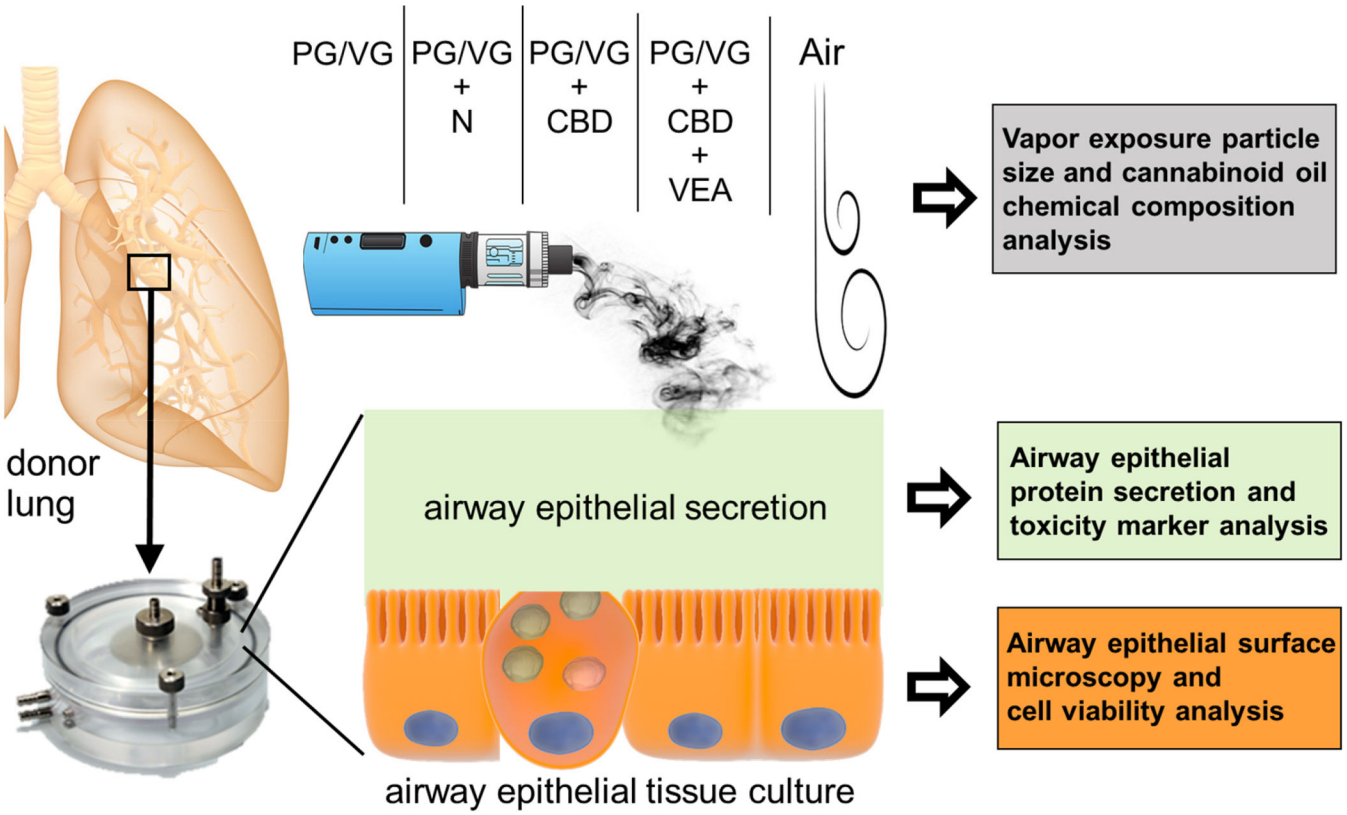

Figure 1: Schematic of the experimental setup to investigate the impact of CBD oil and VEA containing e-cigarette aerosols:

Primary human bronchial epithelial cultures that were established from donor lungs and grown at the air liquid interface were exposed to air, and aerosols generated by a third generation ENDS device containing either PGVG, PG/VG + nicotine, PG/VG + CBD oil, or PG/VG + CBD oil + VEA in 3 exposure sessions with 24 h intervals. Poste-exposure HBE cultures were analyzed by light microscopy, cell viability assessment and secretion proteomics.

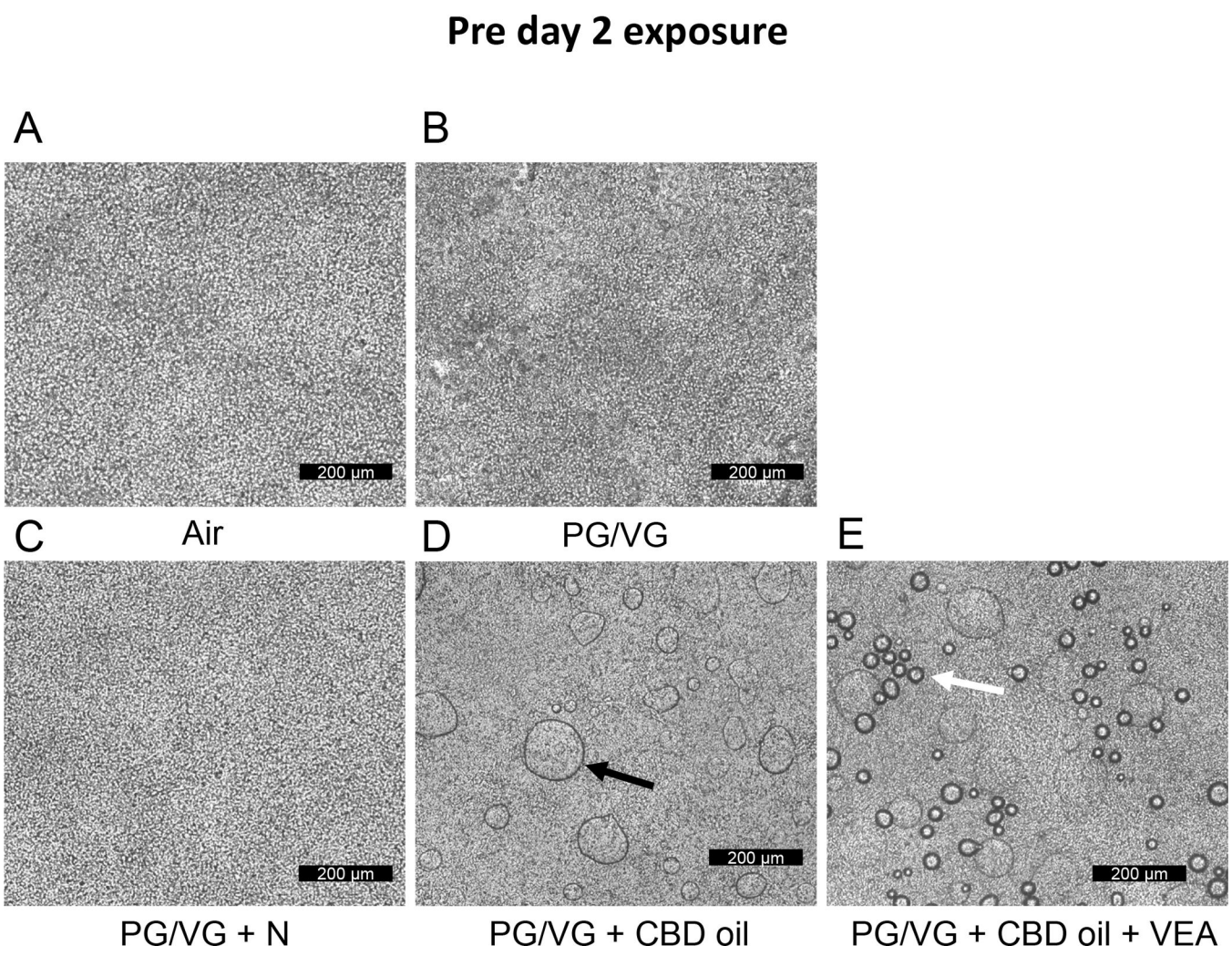

Figure 2: Aerosolized CBD oil and VEA accumulate on HBEC apical surfaces pre day 2 exposures.

Transmission light micrographs acquired from HBE culture inserts exposed to (**A**) air, (**B**) PG/VG, (**C**) PG/VG + nicotine, (**D**) PG/VG + CBD oil, and (**E**) PG/VG + CBD oil + VEA. Representative images were collected from n=6 biological replicate cultures per exposure condition. The black arrow in (**D**) indicates droplet accumulation on PG/VG+CBD oil-exposed cultures. The white arrow in (**E**) indicates droplet accumulation on PGVG+CBD oil+VEA-exposed cultures. Scale bar = 200 µm.

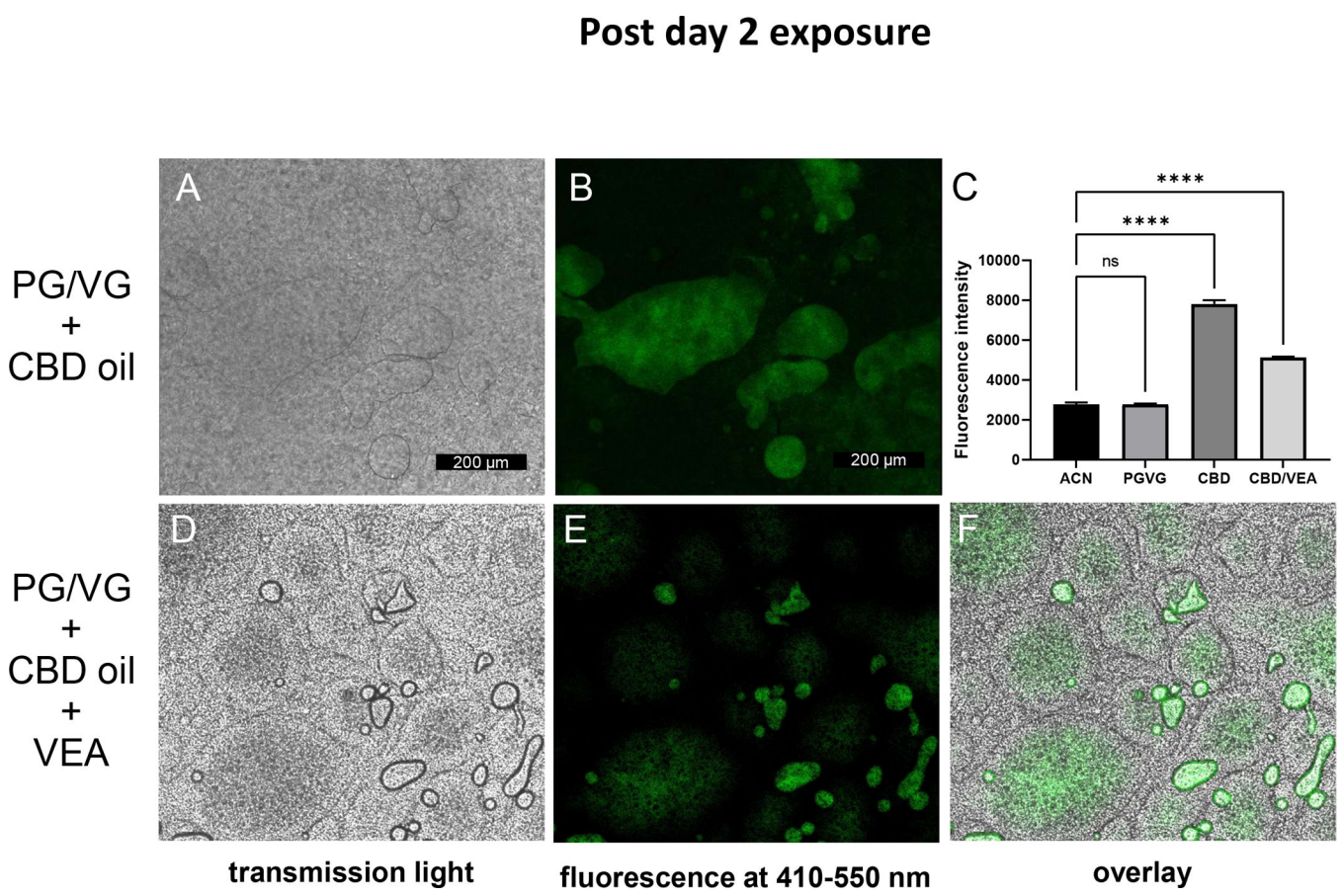

Figure 3: Aerosolized CBD oil and VEA accumulate on and in HBE cultures 2 h post day 2 exposures.

HBE culture insert exposed to PG/VG plus CBD oil, (**A**) transmission light micrograph, (**B**) fluorescence at 410–550 nm. (**C**) Plate reader fluorescence intensities of diluted e-liquids in solvent acetonitrile (ACN). HBEC inserts exposed to PG/VG + CBD oil + VEA. Bar graphs present means and standard deviation values are indicated by horizontal bars. Statistical significance was determined by ANOVA and multiple comparison analysis, and the p-value is indicated by **** ≤ 0.001. (**D**) Transmission light micrograph, (**E**) fluorescence at 410–550 nm, and (**F**) overlay. Representative images were collected from n=6 biological replicate cultures per exposure condition. Scale bar = 200 µm.

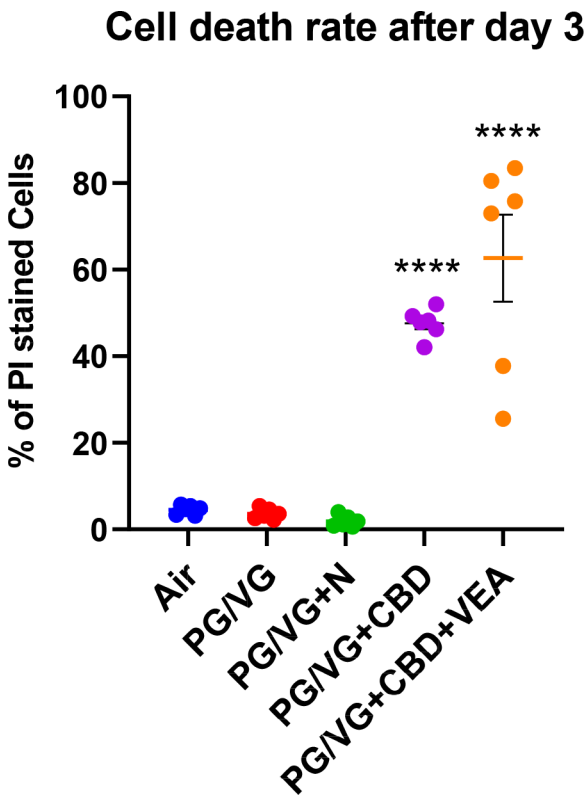

Figure 4: CBD oil- and VEA aerosol-exposed HBECs show high percentages of dead cells after 3 consecutive exposures.

HBECs exposed to aerosols containing CBD oil showed ~45% and CBD oil+VEA ~60% dead cells after the 3rd exposure. Plotted are percentages of propidium iodide (PI)-positive cells, indicating cell death rates for each exposure group. HBE cultures from 6 individual donors (n=6) per exposure group were analyzed in triplicate fluorescence analyses. Mean and SEM values are indicated by major and minor horizontal bars, respectively. Statistical significance was determined by Dunn's multiple comparison test; the p-value is indicated by **** ≤ 0.001.

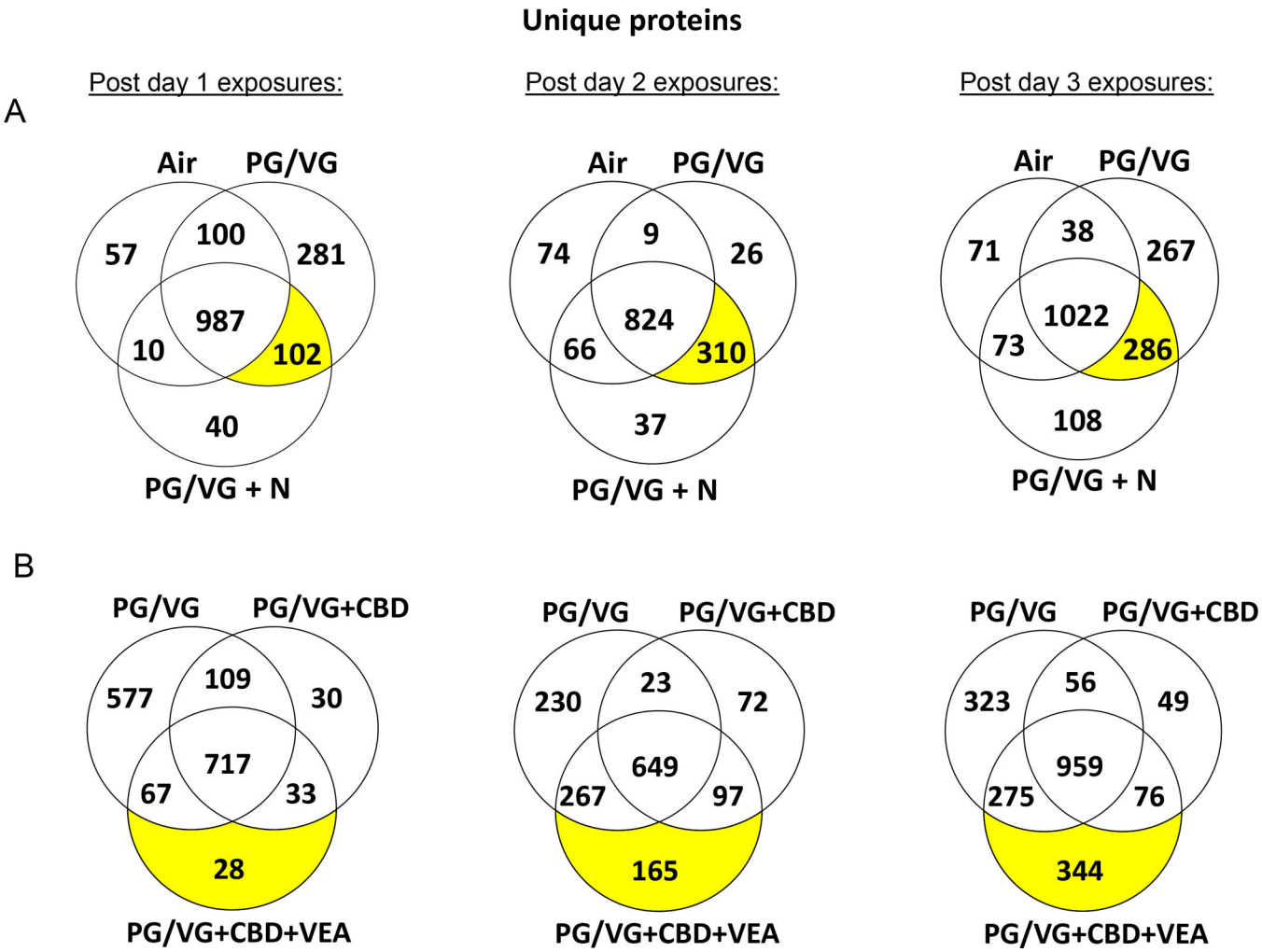

Figure 5: CBD oil, VEA and PG/VG aerosol exposures show differential proteome composition changes in the HBE apical surface liquid.

Venn diagrams show the numbers of uniquely identified proteins in each exposure group and day for (**A**) air versus PG/VG and PG/VG+N and (**B**) PG/VG versus PG/VG+CBD oil and PG/VG+CBD oil+VEA-exposed HBE cultures. The analysis of the uniquely identified protein distributions shows that PG/VG alone, PG/VG+CBD oil and PG/VG+CBD oil+VEA each had unique effects on the proteomic composition of the HBE apical surface liquid.

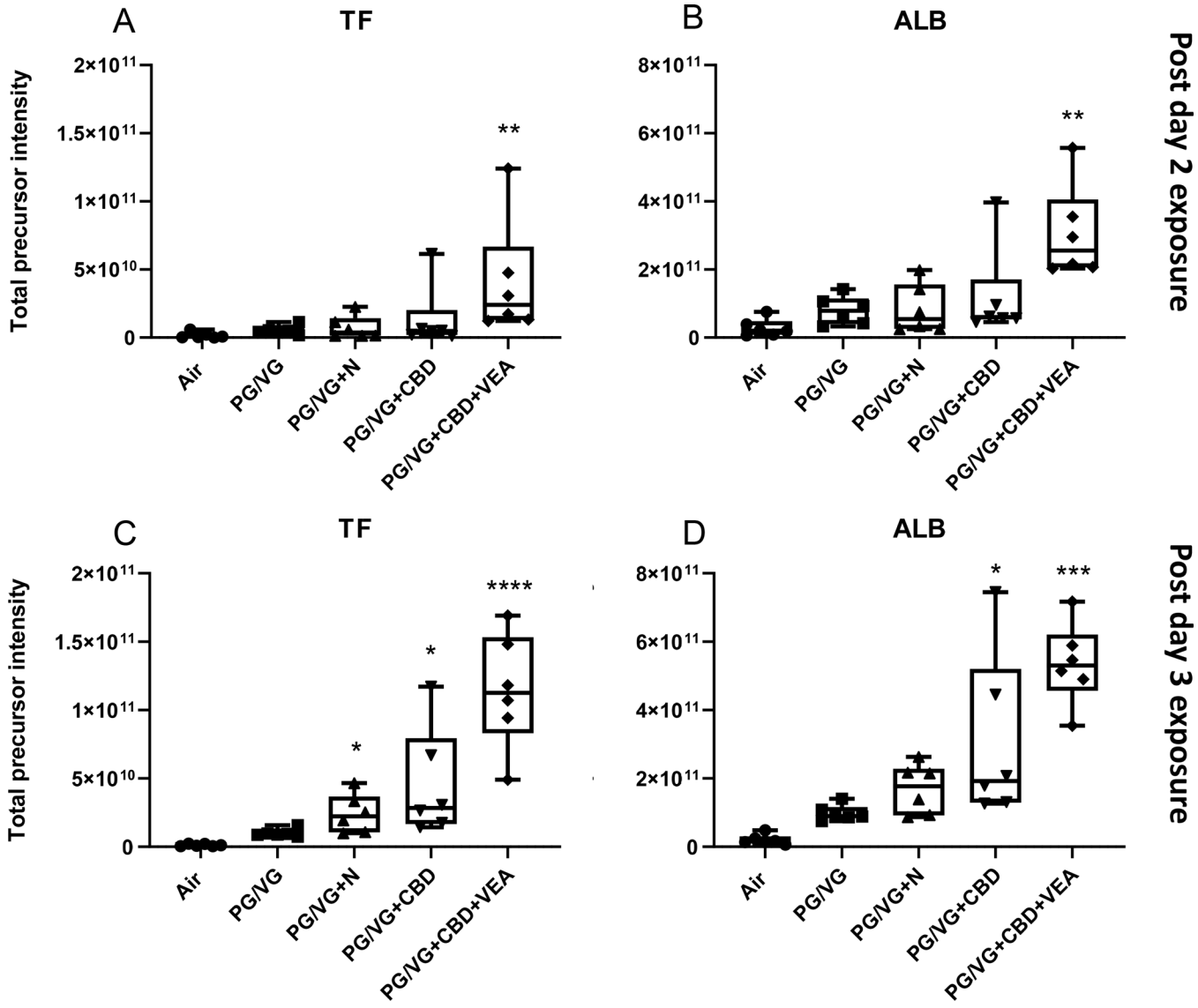

Figure 6: CBD oil and VEA containing aerosol exposure compromise the airway epithelial barrier.

The basal medium exclusive protein (**A**) serotransferrin (TF) and (**B**) serum albumin (ALB) were significantly increased post 2 day exposures with PG/VG+CBD oil+VEA. After the 3rd exposure, (**C**) serotransferrin (TF) and (**D**) serum albumin (ALB) showed further increased levels after PG/VG+CBD oil+VEA in addition to significant increases after PG/VG+CBD oil. Total precursor intensities in each panel are the sums of precursor peptide ion intensities for a given protein, used to assess the presented protein abundances. The mean and SEM values are indicated by major and minor horizontal bars, respectively. Statistical significance was determined by Friedman's nonparametric test and Dunn's multiple comparison analysis. The p-value is indicated by * ≤ 0.05, *** ≤ 0.005, **** ≤ 0.001.

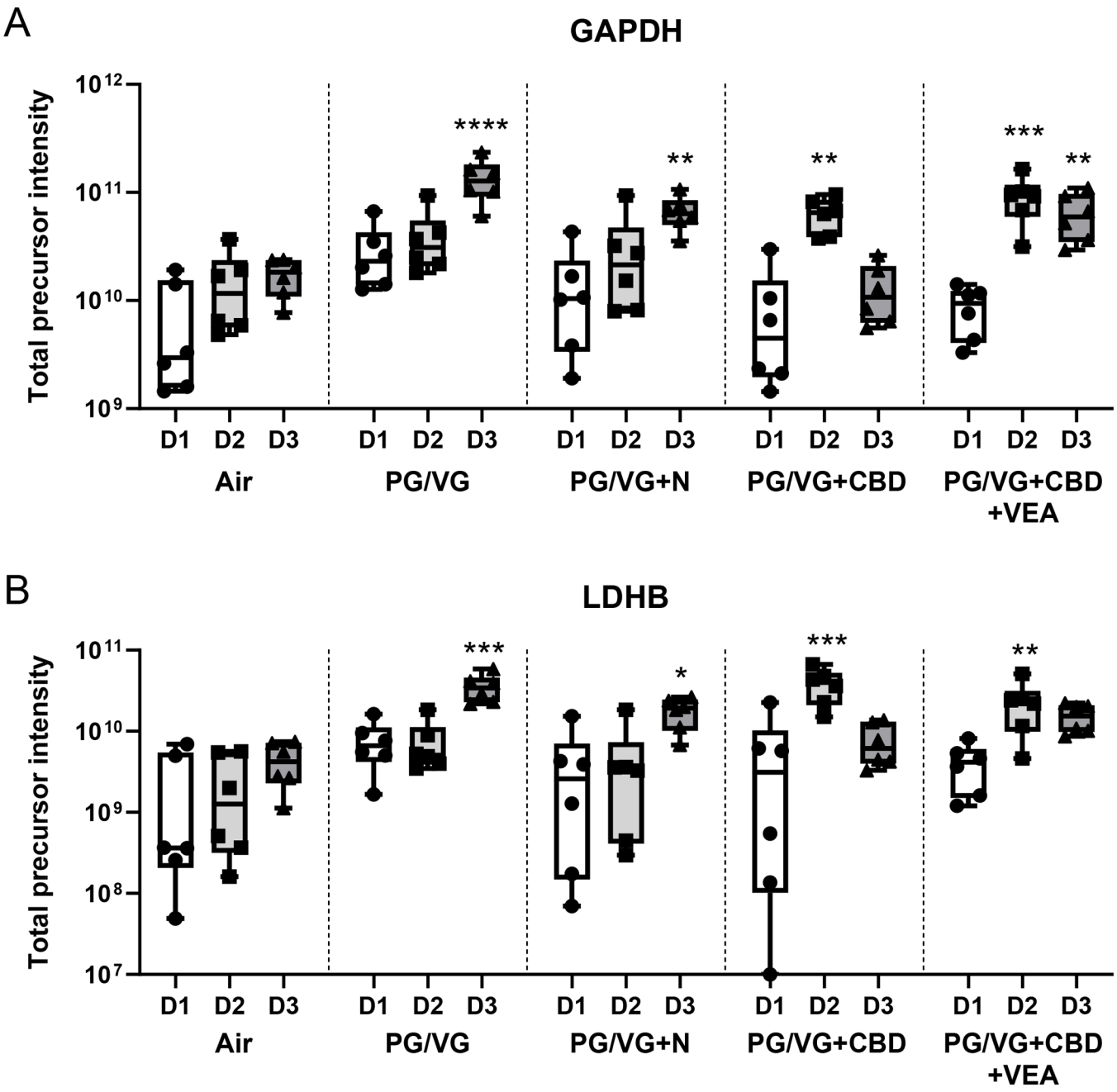

Figure 7: PG/VG, CBD oil and VEA aerosol exposure causes leakage of cytosolic proteins and cytotoxicity markers GAPDH and LDH from HBE cells.

The typical cytosolic proteins (**A**) glyceraldehyde-3-phosphate dehydrogenase (GAPDH) serotransferrin and (**B**) lactate dehydrogenase (LDH) were significantly increased after the 3 day exposure to PG/VG and PG/VG+N. PG/VG+CBD oil- and PG/VG+CBD oil+VEA-exposed cultures displayed the highest apical surface liquid levels after the 2nd exposure, indicating an earlier toxicity impact. Total precursor intensities in each panel are the sums of precursor peptide ion intensities for a given protein, used to assess the presented protein abundances. Mean and SEM values are indicated by major and minor horizontal bars, respectively. Statistical significance was determined by Friedman's nonparametric test and

Dunn's multiple comparison analysis, and the p-value is indicated by * ≤ 0.05, ** ≤ 0.01, *** ≤ 0.005, **** ≤ 0.001.

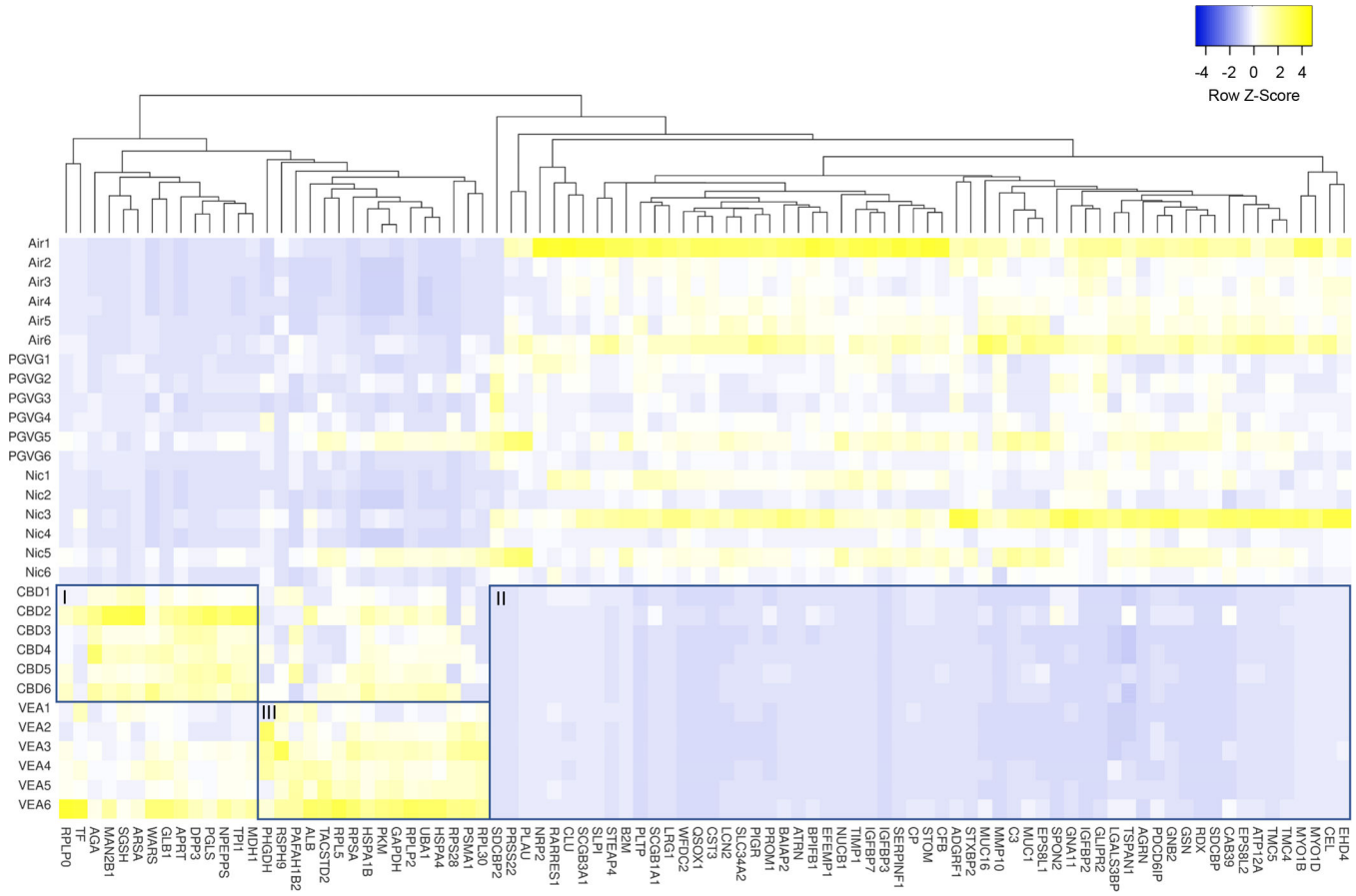

Figure 8: Heatmap of proteins that displayed significantly altered levels in the HBE apical lining fluid after PG/VG+CBD oil+VEA aerosol exposure.

The heatmap includes 91 proteins that were selected based on their significant ($p<0.05$) difference in abundance between PG/VG and PG/VG+CBD oil+VEA after the 2nd exposure, as determined by the Wilcoxon signed rank test. Among clustering areas, three are highlighted by rectangles labeled I, II and III.

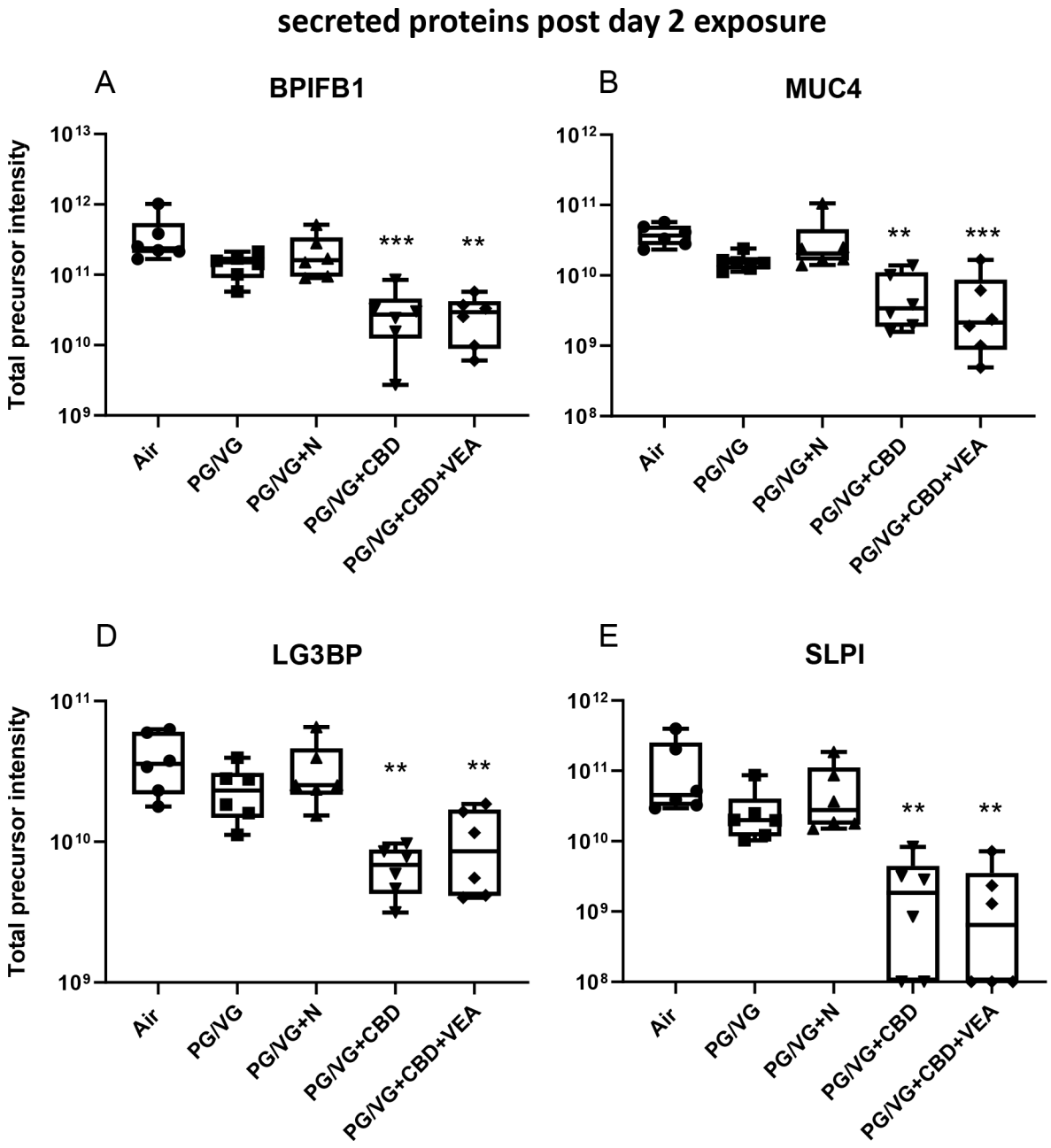

Figure 9: CBD oil and VEA aerosol exposure causes significant reductions in major secreted airway proteins.

The relative proteomic quantification of major secreted proteins in the HBE lining fluid. (**A**) BPI fold containing family B member 1 (BPIFB1), (**B**) mucin 4 (MUC4), (**C**) galectin 3 binding protein (LG3BP) and (**D**) secretory leukocyte peptidase inhibitor (SLPI) showed significant reductions after CBD oil or VEA containing aerosol exposure. Total precursor intensities in each panel are the sums of precursor peptide ion intensities for a given protein, used to assess the presented protein abundances. The mean and SEM values are indicated by major and minor horizontal bars, respectively. Statistical significance was determined by

Friedman's nonparametric test and Dunn's multiple comparison analysis, and the p-value is indicated by ** ≤ 0.01, *** ≤ 0.005.

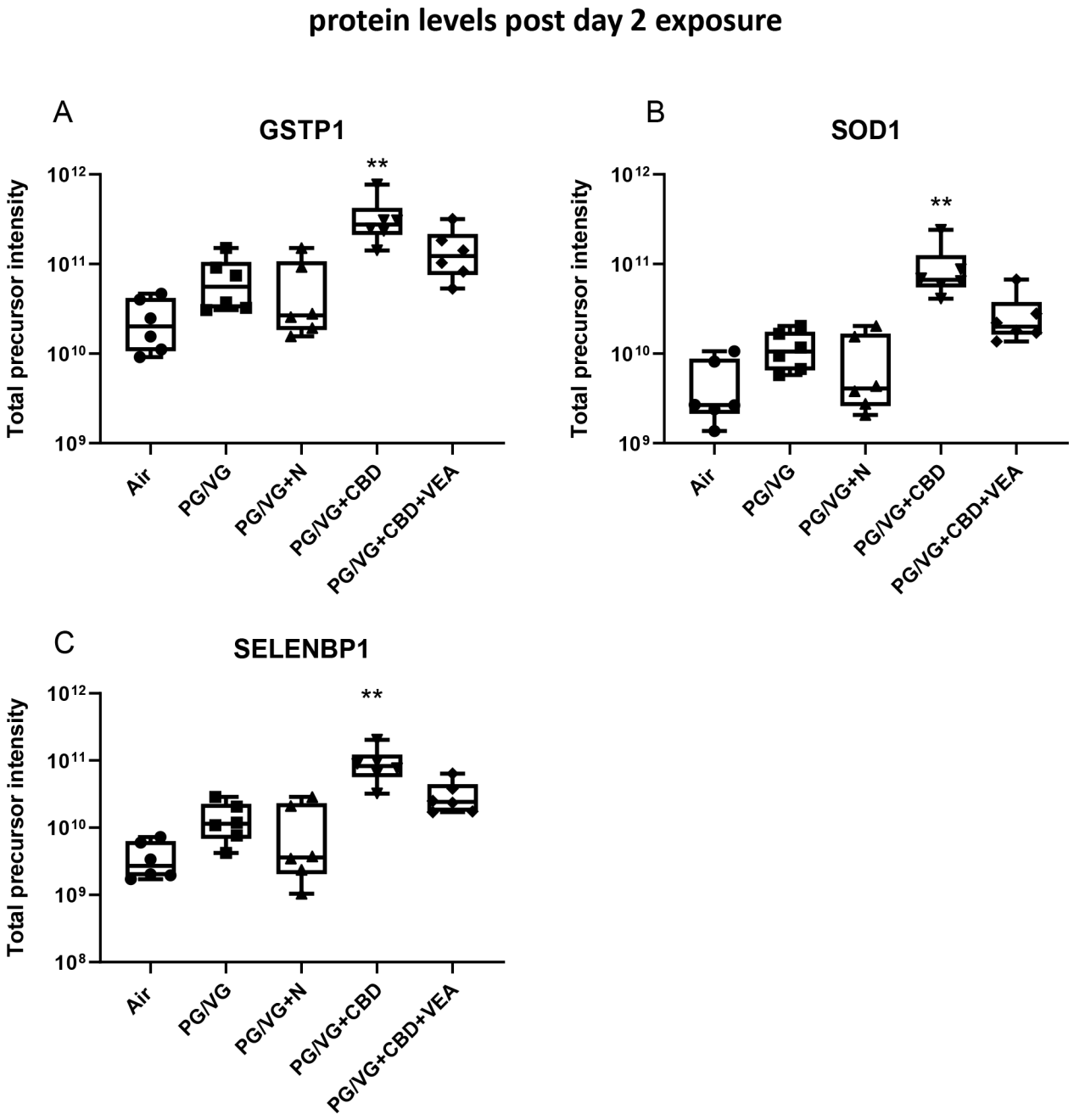

Figure 10: CBD oil containing aerosol exposure results in increases in detoxifying and redox stress proteins in the airway epithelial lining fluid.

The proteins (**A**) glutathione S-transferase P1 (GSTP1), (**B**) superoxide dismutase 1 (SOD1), and (**C**) selenium binding protein 1 (SELENBP1) showed significant increases after CBD oil aerosol the 2 day exposure. Total precursor intensities in each panel are the sums of precursor peptide ion intensities for a given protein, used to assess the presented protein abundances. The mean and SEM values are indicated by major and minor horizontal bars, respectively. Statistical significance was determined by Friedman's nonparametric test and

Dunn’s multiple comparison analysis, and the p-value is indicated by ** ≤ 0.01, *** ≤ 0.005.